

Comparative Analysis of Process Stability in PBF-LB/M: (Thermal) Highspeed Imaging vs. Melt Pool Monitoring using Novel Gas Mixtures

T. Deckers^{A,B}, F. Wolf^A, P. Forêt^A, G. Witt^B, S. Kleszczynski^{B,C}

^A Linde GmbH, Linde Technology- Additive Manufacturing, Germany

^B Institute of Product Engineering, Chair of Manufacturing Technologies, University of
Duisburg-Essen, Germany

^C Center for Nanointegration Duisburg - Essen (CENIDE), University of Duisburg-Essen,
Germany

Keywords: Process Monitoring, Highspeed Monitoring, Thermal Highspeed Monitoring, Process Gas, Helium, Alloy 718

Abstract

Powder bed fusion of metals using a laser beam (PBF-LB/M) is increasingly gaining popularity in the industry. However, ensuring a consistent quality of parts processed by PBF-LB/M is crucial to compete with established manufacturing processes. In-situ process monitoring systems, such as coaxial melt pool monitoring (MPM), can contribute to this goal by minimizing post-process quality control. Three monitoring systems, a commercially available MPM system, an optical high-speed camera, and a thermal high-speed camera, were compared to identify process phenomena. Secondly, the suitability of the MPM system for in-situ quality control was tested by employing novel gas mixtures in the process. The mixtures include argon (Ar) with hydrogen (H₂), helium (He), and carbon dioxide (CO₂). The first results showed the capabilities of the MPM system to monitor relevant process anomalies. Also, the addition of He and H₂ to the process gas resulted in an improvement in the melt pool stability and a reduction of process by-products compared to Ar.

Introduction

Additive Manufacturing (AM) is used more frequently in the industry to produce complex parts [1]. This manufacturing technology is already the standard for special applications in the medical or aerospace industry [2, 3]. Compared to conventional manufacturing processes, AM offers the freedom of design and functional integration. This is essential to meet the increasing requirements of the industry in terms of parts and the cost-effectiveness of individual projects [4]. One of the most widespread AM technologies is a process called powder bed fusion of metals using a laser beam (PBF-LB/M) [5]. In this process, a metallic powder is distributed by a recoater (R) and melted locally layer-wise by the energy of a laser source [5]. A protective gas-shielded process chamber is crucial to ensure consistently high process stability and part quality. This atmosphere limits the oxidation and nitriding reactions of the powdered material and the melt pool. Dietrich et al. [6] stated that a minimum residual oxygen content of 1000 ppm (typically the lowest machine standard) is insufficient for processing titanium and its alloys. Puzon et al. [7] supported this thesis and investigated various alloys and their part properties at residual oxygen contents below ten ppm. Another function of the process gas consists of the continuous recirculation of the gas above the build platform, ensuring the removal of process by-products from the interaction zone of the laser. Ladewig et al. [8] studied the influence of the gas flow speed and the resulting process stability and part quality. The authors indicated that a low gas speed leads to low laser coupling due to process by-products. Reijonen et al. [9] could confirm this phenomenon. Furthermore, the process gas has also been identified in various publications as a new individual process parameter in addition to

the conventional laser parameters [10-14]. In PBF-LB/M, nitrogen (N₂) or argon (Ar) are commonly used, depending on the material [15]. Novel process gas mixtures containing helium (He) or hydrogen (H₂) in Ar are being studied. Bidare et al. [12] compared printing in Ar and He high-pressure atmospheres. Besides a reduced recoil pressure due to the high-pressure atmosphere, using He led to less formation of process by-products. Pauzon et al. [16] were able to increase productivity and part quality on Ti - 6Al - 4V by adding fractions of He to the process gas. Deckers et al. [11] identified a reduction in surface roughness and increased part density using alloy 718. Thus, a process influence can be generated via the type of protective gas, its velocity, its flow profile, or the chamber pressure. As a wide range of process influences exist, a constantly reproducible part quality must be ensured for an industrial application. This can be verified through process monitoring. A distinction is made between in-situ and subsequent monitoring. The present study focuses on in-situ monitoring. In-situ monitoring can be differentiated into on-axis and off-axis systems. On-axis systems like the commercially available EOSTATE melt pool monitoring (MPM) acquire emission data within the laser beam path via beam-splitting mirrors [17]. The acquired data depends on the implemented sensor type. For example, single-channel sensors such as photodiodes, pyrometers, or high-speed cameras are commonly used [18-20]. On the contrary off-axis monitoring captures process information at a fixed angle [19]. Thus, it can be used to validate on-axis data. MPM offers a high temporal (60 kHz) and spatial resolution (50 μm/pixel) [17]. However, little knowledge about the correlation between the digit sensor signal and the influence of process phenomena is available. Stutzman et al. [20] investigated optical emissions during PBF-LB/M changing the gas flow speed. Felix et al. [21] correlated the MPM sensor signal with part defects but did not analyze the influences of the signal. Due to MPM spot size, the measurement is influenced by many different process phenomena, such as process by-products (spatter, fumes,..), the solidified material, the powder bed, and the melt pool. These influences are to be differentiated and analyzed with two off-axis setups within this paper. In addition, the influence of novel process gas mixtures will be assessed with MPM and two custom-built monitoring systems.

Materials and Methods

PBF-LB/M Process

The experiments were carried out using an EOS (Electro Optical Systems GmbH, Germany) M290 PBF-LB/M system. In addition to a melt pool monitoring system from EOS, custom-made monitoring systems were installed. The material used was alloy 718 with a 22 - 44 μm particle size distribution provided by Praxair Surface Technologies. The process parameters were optimized based on the commercially available alloy 718 EOS process parameters for a layer thickness of 40 μm. In order to meet the industry's demand for increasing productivity, the study was conducted not only with the standard layer thickness of 40 μm but also with adapted process parameters and a layer thickness of 120 μm. Table 1 lists the utilized process gas mixtures with an excerpt of their physical properties. The gas speed of an EOS M290 is controlled by differential pressure in the central gas ductwork. Thus, the differential pressure had to be determined with respect to the physical properties of each process gas mixture. This ensures an equal and uniform gas flow and speed (G). A build plate was equipped with several measuring points in the preceding study. These points were analyzed using different differential pressures utilizing a Testo 416 vane anemometer. The differential pressure for gases with a He-content higher than 50% had to be adjusted. Before each of the six print jobs, the chamber volume was opened and re-purged three times with the respective gas to ensure a full exchange of the process atmosphere. To safely use gases containing H₂, the ADDvance[®] O₂ Precision was used. This

device analyzes and controls the oxygen and humidity level inside the process chamber and is unaffected by H₂.

Name	Density in kg/m ³	Thermal Conductivity λ in W/(m*K)	Specific heat capacity c_p in J/(kg*K)
Ar	1.78	0.02	0.52
He	0.18	0.15	5.19
Ar + 30%He	1.30	0.04	0.71
Ar + 70%He	0.66	0.08	1.41
Ar +30%He +10%CO ₂	1.32	0.04	0.76
Ar +5%H ₂	1.70	0.02	0.57

Table 1: Physical properties of the employed gases at norm conditions ($p=1.013$ bar, $T=0^\circ\text{C}$).

The job design consists of three cuboid specimens (10 x 10 x 10 mm). Three single scan tracks (SL) are on top of each specimen. The length of each SL is 10 mm.

Process Monitoring

Thermal High-Speed Setup

Initially, the process of an EOS M290 can only be observed by the laser-safety window located at the machine's front door. This window contains a safety glass that filters the radiation of the laser beam at 1064 nm. To utilize a thermal high-speed (THS) camera, a window with a different transmission wavelength band had to be used. Hence, an additional observation area was necessary. Therefore, an unused cable feedthrough at the top of the build chamber was modified. A specific infrared long-pass filter was chosen with a transmission wavelength band of $\lambda=2.5 - 4.8 \mu\text{m}$ to observe the process with a THS camera. The filter was placed in a custom-made aluminum mount, which fit into the cable feedthrough. Since the filter is not sufficient protection against reflection laser radiation, an additively manufactured 316L stainless steel cover was installed between the camera and the aluminum filter housing. The setup-up, highlighted in Figure 1, allowed safe monitoring of a circular area. The approximate diameter is 50 mm near the gas inlet on the build platform.

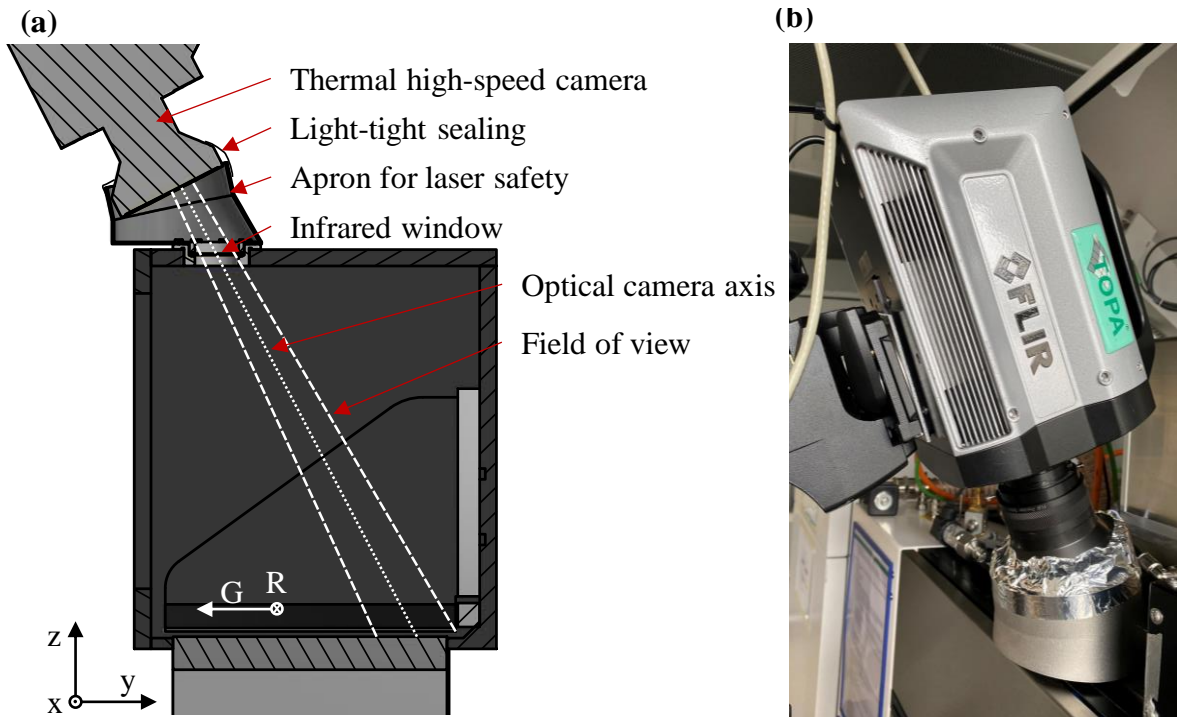


Figure 1: Schematic layout of the THS study (a) and final experimental setup (b).

A FLIR X6900sc THS camera with a 100 mm focal distance lens was used. A 3/4 - inch spacer ring was used between the camera and the lens. This enabled to control the focus on the process zone. The camera was mounted on a tripod in front of the M290. To run the camera, the software FLIR ResearchIR 4 was utilized. This software facilitates camera control and allows for adjustments to various settings. The trials were recorded with and without a neutral density (ND) filter at a 320 x 256 pixels resolution to allow the camera's maximum framerate of 1956 Hz. If FLIR superframing was used, the framerate was set to 862 Hz. Since the emissivity within the PBF/LB-M process is unknown and subject to ongoing research, an alternative approach was made to compare the monitored temperature. It was assumed that the emissivity coefficient within the study remains the same regardless of the process gas. Thus, the process gas is the only changing variable. A custom MATLAB-based script processed the videos, normalized them, and plotted them side-by-side. The temperature values are normalized using the upper and lower limits of the corresponding temperature range employed during a specific recording.

High-Speed Setup

Using a high-speed (HS) camera for process monitoring positioned in front of the laser safety glass at the front door is not ideal due to the resulting viewing angle. Therefore, an existing recess on the right side of the build chamber was modified, in which an LED for the illumination is located. A fully transmissible glass plane was initially used to cover the original LED light source. This pane was exchanged for a laser safety glass equivalent to the one mounted in the process chamber door. A light source consisting of three 32 - Watt LED panels had to be installed in the build chamber near the ceiling. Especially for HS cameras, bright illumination is necessary due to the fast shutter speed. The additional light allowed an increase in the frame rate. The camera, a Photron FASTCAM NOVA S 12, and a deflection mirror were placed on a mounting rail to adjust the viewing angle and focus. A Nikon Micro-Nikkor 200 mm 4,0 D IF-ED lens was attached to the HS

camera. The framerate was set to 4000 Hz with a shutter speed of 1/16000 seconds at a resolution of 1024 x 1024 pixels. The recording was controlled with the Software Photron FASTCAM Viewer 4 and exported to MATLAB for further custom analysis. The HS setup, displayed in Figure 2, ensures an observation of the process perpendicular to the gas flow. After recording, the videos were further processed and plotted using MATLAB.

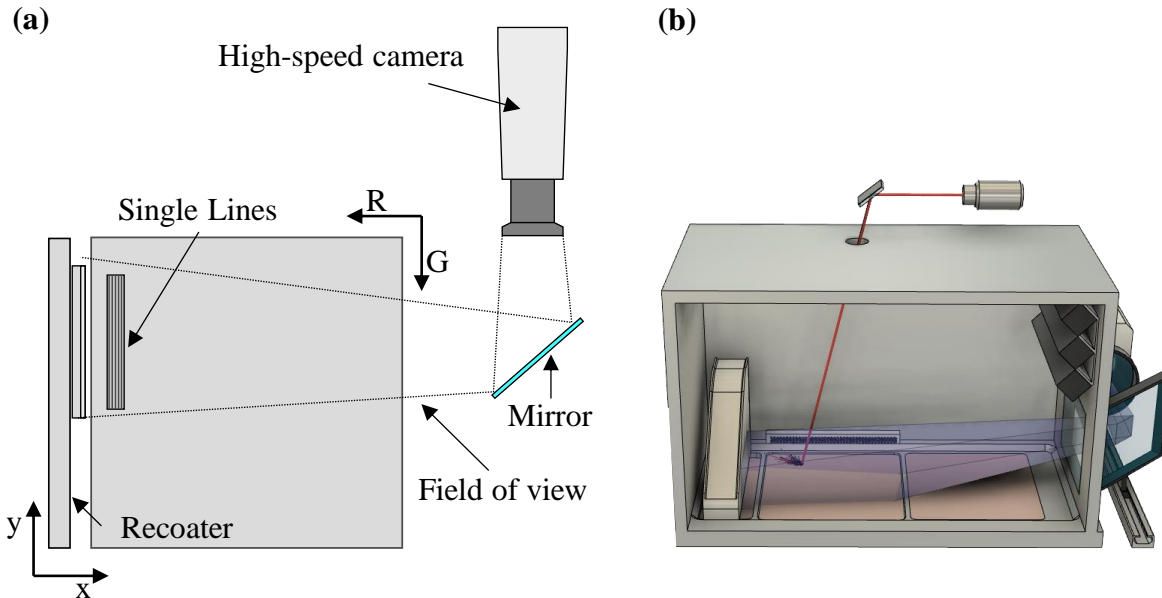


Figure 2: Schematic layout of HS setup (a) and CAD mock-up (b).

Evaluation for MPM

A custom methodology was developed to gain a further understanding of the MPM signal. Firstly, influences on the sensor's signal data had to be investigated to make correlations between the signal data and the process phenomena. Prior to the measurements, the EOSTATE MeltPool system had to be calibrated to ensure a precise measurement of the geometrical and intensity data. Preliminary studies were conducted to gain a deeper understanding of the process gas impact on the MPM. This preliminary study involved the recording of the MPM signal varying the laser power. Within the main study, only the process gas was changed. After each print job, the respective MeltPool raw data was exported. A workaround had to be used since the raw data could not be acquired from the EOS software. First, the data of each layer was exported as .fig files. This data includes the x & y-position of the laser focus spot, the on & off-axis intensity measured by the photodiode, the exposure type, the modulation signal, and the laser power. The data of each layer was then converted to a MATLAB-based matrix representation for further processing. A custom-made MATLAB APP was created to display, segment, analyze, and export the acquired data according to the requirement. The MPM, the MPM data, and the workflow are shown in Figure 3. Only a small part of the custom software was used for the present study. This part exported and plotted the intensity profiles of the single lines, comparing the effect of the different gas atmospheres.

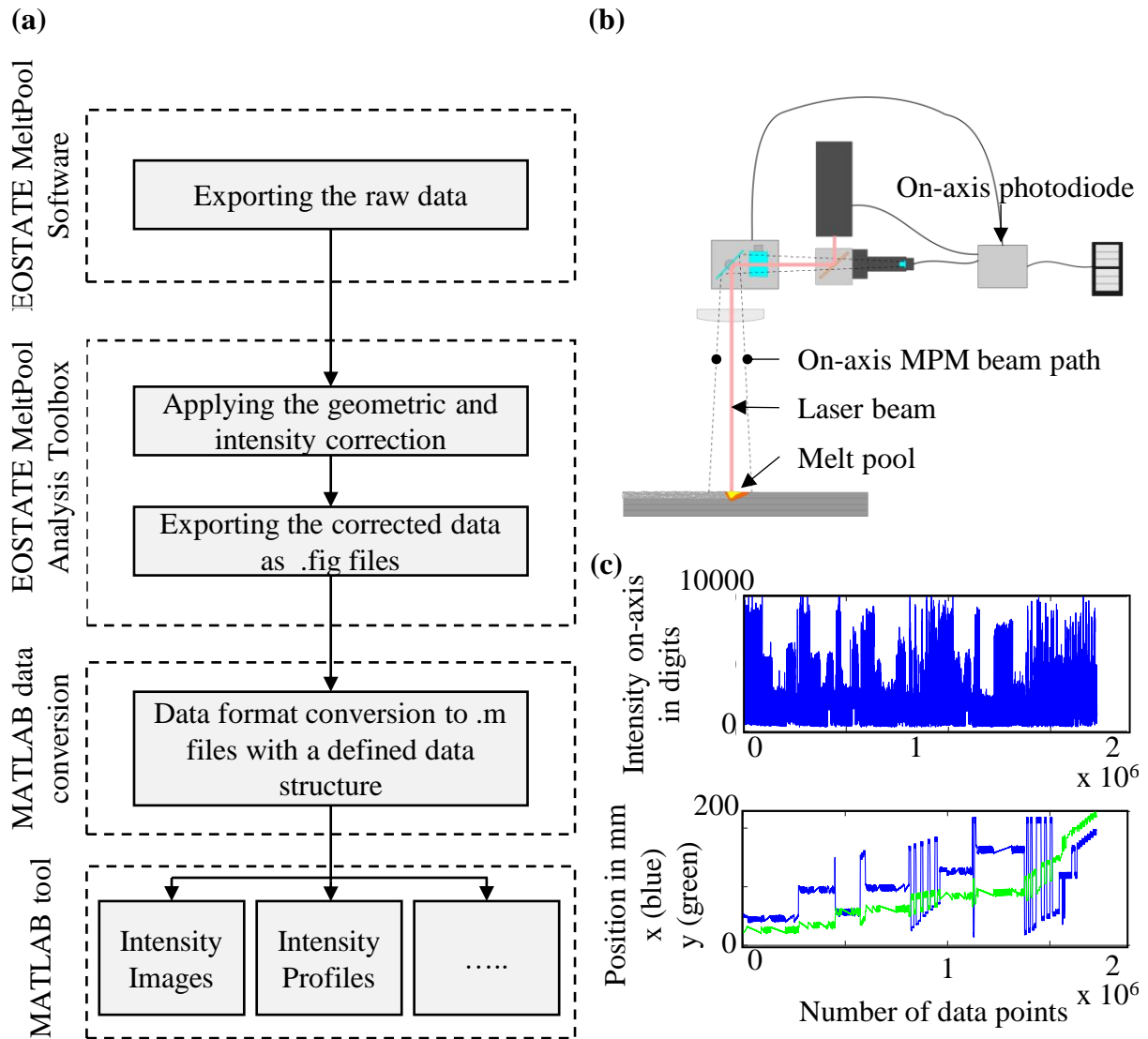


Figure 3: Workflow to evaluate MPM data (a), the schematic layout of MPM (b) with its corresponding raw data (c).

Results and Discussion

Thermal High-Speed Analysis

The custom setup employed enabled the thermal observation of the PBF-LB/M process. With the ND filter activated, the recording was limited to high-temperature observations. Therefore, the melt pool could be analyzed as unsaturated. It was observed that increasing the He or H₂ content led to a decrease in the melt pool surface temperature. This observation was made by comparing the maximum normalized temperatures in a 20-pixel region of interest (ROI) around the melt pool of the 40 μm layer thickness single lines. The results are displayed in Figure 4. This might be due to an increased heat capacity and conductivity of the novel gas mixtures compared to an Ar-atmosphere.

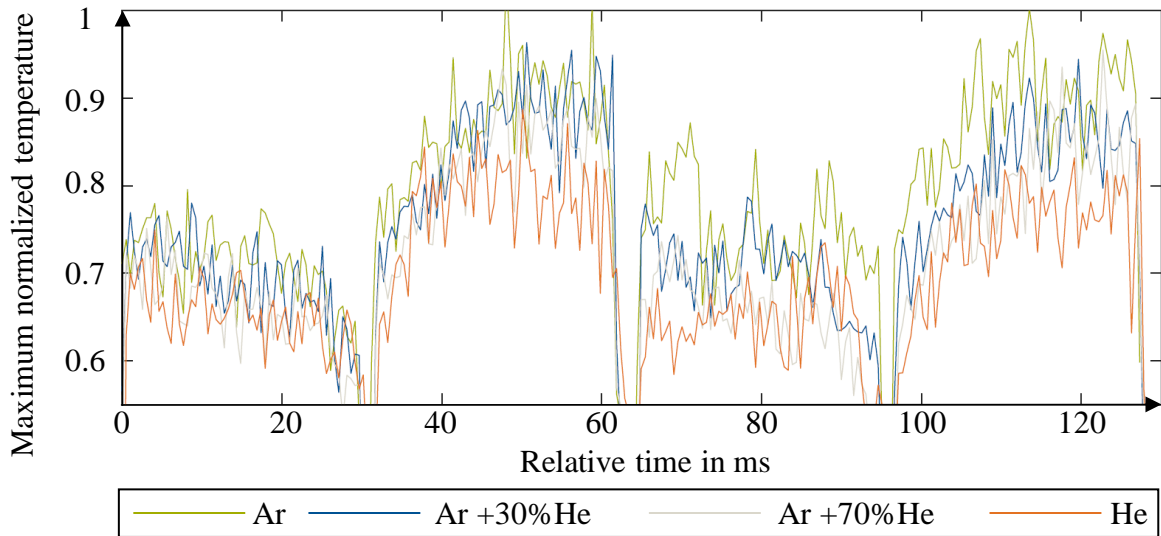


Figure 4: Comparison of the normalized maximum temperature of the THS camera.

Without the ND filter, the melt pool size, its cooling behavior, the process by-products, and their temperature profile could be made visible. If one compares the synchronized frames, it is apparent that the process gas significantly influences the amount and temperature of process by-products. This effect is also present at a 40 μm layer thickness.

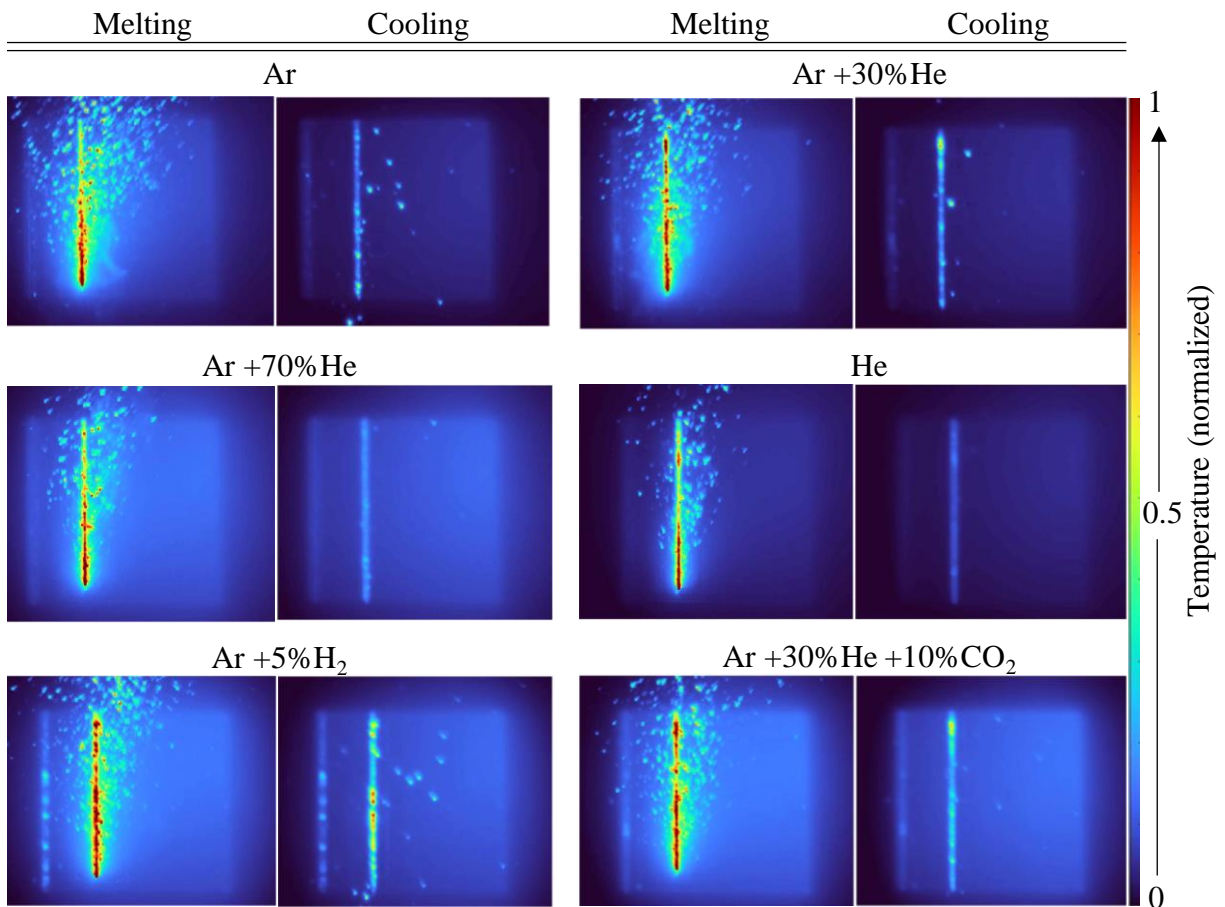


Figure 5: Sequence of synchronized THS videos at the melting and cooling stage.

This is already visible using a layer thickness of 40 μm . He- and H₂-containing atmospheres create fewer process by-products and significantly reduce their temperature. Using pure He doesn't even create high-temperature by-products, based on the pseudocolor image in comparison to pure Ar. This could be caused by a change in the recoil pressure or the thermal properties. Due to the fast cooling, particle adherence to solid surfaces is also greatly influenced. This correlates with the findings of Deckers et al. [11] for an improved surface quality using He- or H₂-containing gases. As the layer thickness increased, the occurrence of process anomalies also rose. This effect is due to an increase in laser-powder interaction. There was a glowing behavior of the melt pool under the Ar-atmosphere notable. Within the 120 μm study, a balling effect (unstable, discontinuous melt pool tracks) for pure Ar Ar-H₂ and low Ar-He mixtures could be identified. Mixtures with a He fraction above 30 Vol.-% created homogenous scan tracks even for 120 μm layer thickness. The influence of CO₂-containing mixtures known from Gas Metal Arc Welding (GMAW) did not arise. No increased energy input or significant increase in process by-products was detected using CO₂ containing mixture. This could be due to the present helium content of that mixture.

Meltpool Monitoring Analysis

Generally, the MPM sensor signal data exhibits fluctuations within approximately 10 % of the mean value. The sensor signal is depicted in Figure 6 a). In order to gain a better understanding of the influence of process gases, various laser powers were examined using different process gases. This is evident in Figure 6 b), where higher laser powers correspond to an increase in MPM intensity. This effect is more pronounced at lower laser powers (P_L) and increased the average MPM Intensity ($IS_{MPM, avg}$). For instance, using an Ar atmosphere, increasing P_L by 50 W from 135 W led to an average intensity increase of 882 digits, while the same increase from 285 W caused an average increase of 409 digits. At a P_L of 285 W, the measured $IS_{MPM, avg}$ is 4646 digits for an Ar atmosphere, 4637 digits for Ar+30 Vol.-%, 4429 digits for Ar+70 Vol.-%, and 4243 digits for He. The difference between the pure Ar and He atmosphere amounts to 403 digits, similar to the difference observed with a 50 W increase in P_L . It should be noted that the values displayed in Figure 6 b) are obtained for single scan tracks conducted against the gas flow at 40 μm layer thickness.

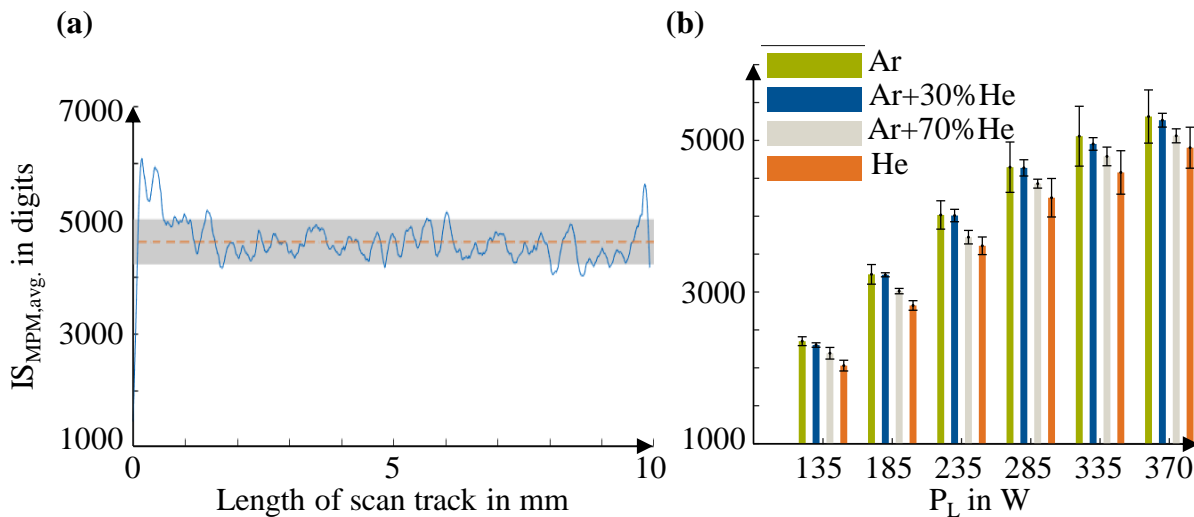


Figure 6: Fluctuation of sensor data for a single scan track (a) and the comparison of the influences of process atmosphere and laser powder on $IS_{MPM, avg}$. (b).

High-Speed Analysis

The HS recordings highlighted, similar to the THS results, a change in the process by varying the process gases. First, an evaluation of the influence of incandescent by-products on the MPM signal was made. Therefore, the MPM intensity was plotted in addition to a frame-wise spatter count algorithm. From Figure 7, it is apparent that a correlation between the MPM signal and the occurrence of process by-products can be made. A significant reduction of signal strength and sensor fluctuation was present using He-containing gases. The Ar-atmosphere created more sensor fluctuation and by-products.

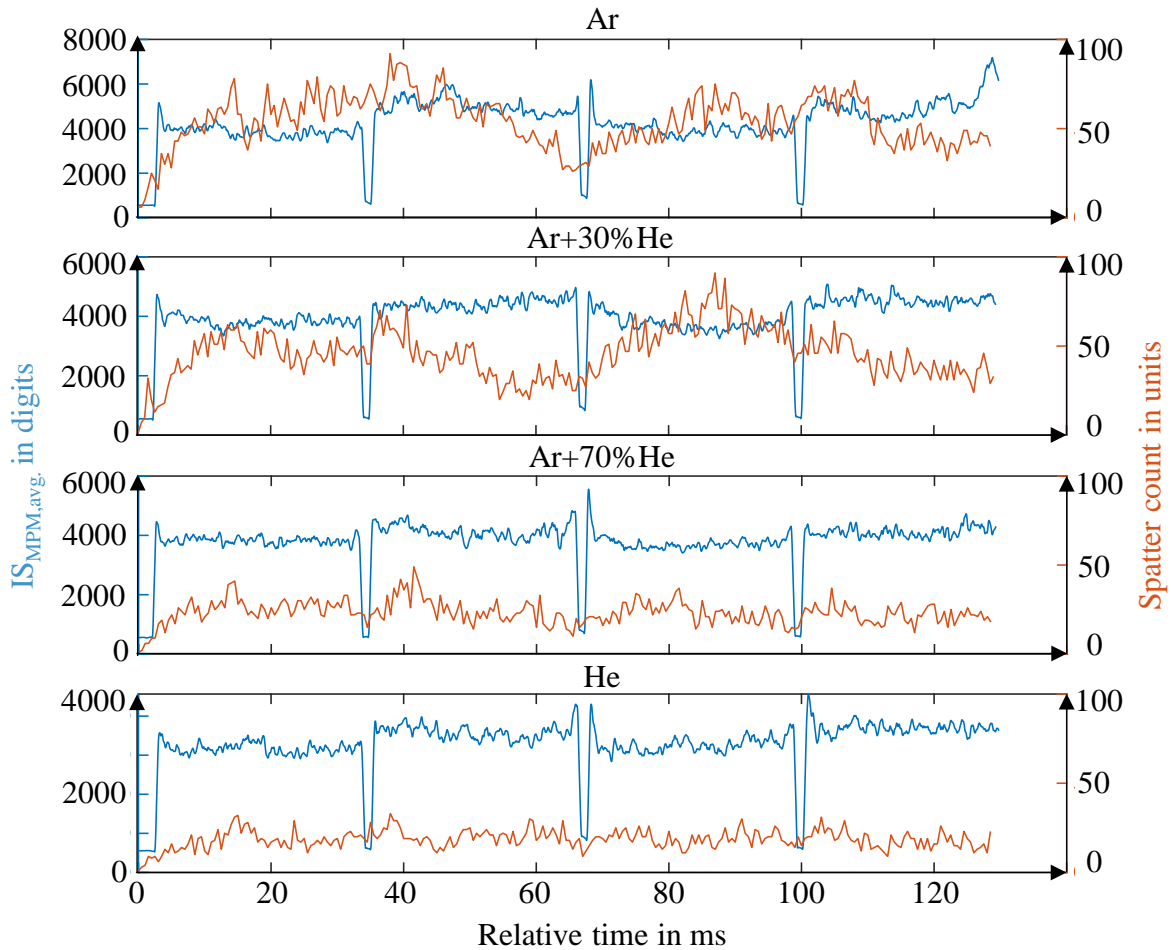


Figure 7: Comparison of $IS_{MPM,avg.}$ and the spatter count using different process atmospheres.

Additionally, if zoomed to a field of view (FOV) of the melt pool, the process fume could be investigated. The FOV of the employed process atmospheres are displayed in Figure 8. The He-enriched atmospheres seemed to have decreased fume density. Furthermore, the removal of fumes was affected by the process gas used. High He contents above 50 Vol.-% created swirls in comparison to a more straight laminar flow of Ar and Ar+30 Vol.-% He. This could be caused due to an insufficient flow speed. Interaction with the laser beam and the fumes were visualized for Ar and low He-containing gases. Since the fume density was visually analyzed, no direct correlation to the MPM signal was made. However, a decrease in MPM signal intensity and a less dense fume behavior are contradictory. Therefore, more intensity could reach the MPM sensor. Thus, the signal

might not be influenced by the generated fumes. Low H_2 and CO_2 mixtures showed no significant influences. They were comparable to Ar +30 Vol.% He.

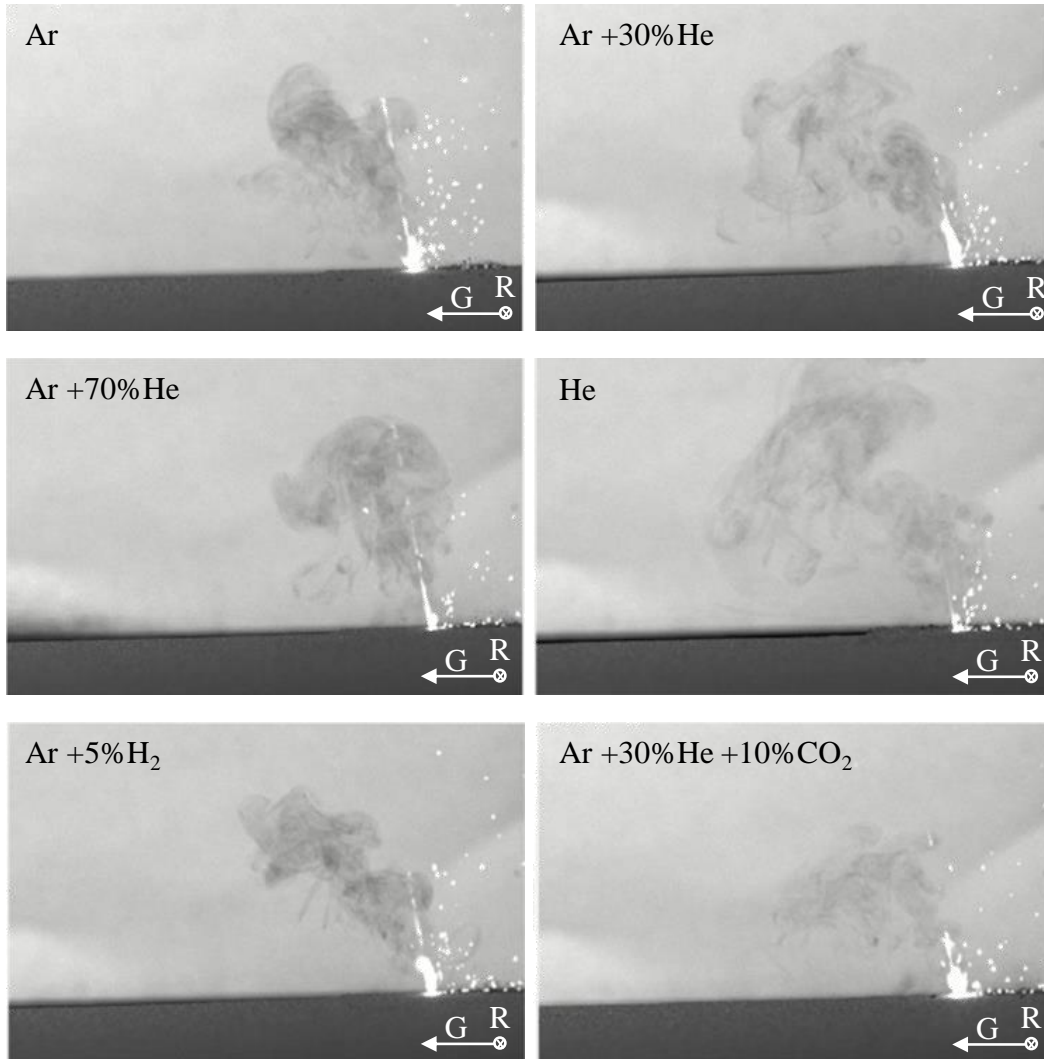


Figure 8: Image Sequence of HS videos to compare process phenomena using different process gases.

Conclusion

Within PBF-LB/M, process stability plays a decisive role in a successful process and the associated part quality. This is challenged by requirements such as increasing productivity and the resulting change in layer thickness or, for example, the identification of new alloys. The present paper analyzed the process stability based on commercially available process monitoring (MPM) and custom monitoring such as THS and HS in an industrial-sized PBF-LB-M machine. He- or H_2 -containing gases offer possibilities to overcome process instabilities and increase part quality. The following conclusions about process monitoring within PBF-LB/M could be made:

- MPM can be used to analyze process stability. This could be validated via a THS setup. However, MPM does not offer the possibility to identify individual process influences due to the measurement spot size and the off-axis recording.

- The MPM signal correlates with laser parameters and the used process atmosphere.
- A custom HS setup could be utilized to monitor the process perpendicular to the gas flow at the level of the process chamber. In addition to the analysis of process by-products, this setup also enables the realization of a schlieren set-up.
- A custom THS setup was implemented to analyze melt pool behavior. This setup facilitates the analysis of melt pool temperatures after further research on the emission coefficient.

The following conclusions about the influence of novel process gases within the PBF-LB/M process could be made. Using novel, He- or H₂-mixtures results in:

- A significant reduction in the generation of spatter and fumes.
- A decrease in MPM surface intensity during welding. This is comparable to a reduction of laser power by 50W.
- Less chance of adherence for hot process by-products. Consequently, the surface quality increases, and surface roughness decreases.
- Faster cooling of the solidifying melt pool surface.
- Fewer interactions of the laser beam with fumes, spatters

Credit author statement

T. Deckers: Conceptualization (lead); Methodology (lead); Investigations (lead); Validation (lead); Visualization (lead); Supervision (lead); Formal analysis (lead); Writing – original draft (lead), F. Wolf: Investigations (supporting); Formal Analysis (supporting); Visualization (supporting), P. Forêt: Supervision (equal), Writing – review & editing (equal), S. Kleszczynski: Supervision (equal), Writing – review & editing (supporting), G. Witt: Supervision (equal).

Declaration of Competing Interest

The authors declare no conflict of interest.

Data availability

The data supporting this study's findings are available from the corresponding author T. Deckers upon reasonable request.

References

- [1] Vaezi, M.; Chianrabutra, S.; Mellor, B.; Yang, S.: Multiple material additive manufacturing – Part 1: a review, In: Virtual and Physical Prototyping, 2013.
- [2] Blakey-Milner, B.; Gradl, P.; Snedden, G.; Brooks, M.; Pitot, J.; Lopez, E.; Leary, M.; Berto, F.; Du Plessis, A.: Metal additive manufacturing in aerospace: A review, In: Materials & Design, 2021.
- [3] Salmi, M.: Additive Manufacturing Processes in Medical Applications, In: Materials (Basel, Switzerland), 2021.
- [4] Wohlers, T. T.; Campbell, I.; Diegel, O.; Huff, R.; Kowen, J.: Wohlers report 2022: 3D printing and additive manufacturing global state of the industry, Fort Collins, Colorado, Wohlers Associates, 2022.
- [5] DIN EN ISO/ASTM 52900:2022-03, Additive Fertigung - Grundlagen - Terminologie (ISO/ASTM 52900:2021); Deutsche Fassung EN_ISO/ASTM 52900:2021, Berlin, Beuth Verlag GmbH.

- [6] Dietrich, K.; Diller, J.; Dubiez-Le Goff, S.; Bauer, D.; Forêt, P.; Witt, G.: The influence of oxygen on the chemical composition and mechanical properties of Ti-6Al-4V during laser powder bed fusion (L-PBF), In: Additive Manufacturing, 2020.
- [7] Pauzon, C.; Raza, A.; Hryha, E.; Forêt, P.: Oxygen balance during laser powder bed fusion of Alloy 718, In: Materials & Design, 2021.
- [8] Ladewig, A.; Schlick, G.; Fisser, M.; Schulze, V.; Glatzel, U.: Influence of the shielding gas flow on the removal of process by-products in the selective laser melting process, In: Additive Manufacturing, 2016.
- [9] Reijonen, J.; Revuelta, A.; Riipinen, T.; Ruusuvoori, K.; Puukko, P.: On the effect of shielding gas flow on porosity and melt pool geometry in laser powder bed fusion additive manufacturing, In: Additive Manufacturing, 2020.
- [10] Traoré, S.; Koutiri, I.; Schneider, M.; Lefebvre, P.; Rodrigues, J.; Dupuy, C.; Coste, F.; Peyre, P.: Influence of gaseous environment on the properties of Inconel 625 L-PBF parts, In: Journal of Manufacturing Processes, 2022.
- [11] Deckers, T.; Ammann, T.; Forêt, P.; Dubiez-Le-Goff, S.; Zissel, K.; Witt, G.: Einfluss heliumhaltiger Prozessgase auf den Laser-Strahlschmelzprozess, In: Zeitschrift für wirtschaftlichen Fabrikbetrieb, 2022.
- [12] Bidare, P.; Bitharas, I.; Ward, R. M.; Attallah, M. M.; Moore, A. J.: Laser powder bed fusion in high-pressure atmospheres, In: The International Journal of Advanced Manufacturing Technology, 2018.
- [13] Pauzon, C.; van Petegem, S.; Hryha, E.; Sin Ting Chang, C.; Hocine, S.; van Swygenhoven, H.; Formanoir, C. de; Dubiez-Le Goff, S.: Effect of helium as process gas on laser powder bed fusion of Ti-6Al-4V studied with operando diffraction and radiography, In: European Journal of Materials, 2022.
- [14] Deckers, T.; Ammann, T.; Forêt, P.; Witt, G.: An Optical Tomography Based Study on the Influence of Different Gases During PBF-LB/M: Distribution of Process By-Products and Part Properties, In: Proceedings of the 18th Rapid.Tech 3D Conference Erfurt, Germany, 17–19 June 2022, 2022, München.
- [15] Pauzon, C.; Hryha, E.; Forêt, P.; Nyborg, L.: Effect of argon and nitrogen atmospheres on the properties of stainless steel 316 L parts produced by laser-powder bed fusion, In: Materials & Design, 2019.
- [16] Pauzon, C.; Forêt, P.; Hryha, E.; Arunprasad, T.; Nyborg, L.: Argon-helium mixtures as Laser-Powder Bed Fusion atmospheres: Towards increased build rate of Ti-6Al-4V, In: Journal of Materials Processing Technology, 2020.
- [17] Fuchs, L.; Eischer C.: In-process monitoring systems In-process monitoring systems for metal additive manufacturing, – EOS GmbH, <https://www.eos.info/en/blog/in-process-monitoring-systems-whitepaper~b~11493> (abgerufen am: 04.07.2023).
- [18] Lott, P.; Schleifenbaum, H.; Meiners, W.; Wissenbach, K.; Hinke, C.; Bültmann, J.: Design of an Optical system for the In Situ Process Monitoring of Selective Laser Melting (SLM), In: Physics Procedia, 2011.

- [19] Yadav, P.; Rigo, O.; Arvieu, C.; Le Guen, E.; Lacoste, E.: In Situ Monitoring Systems of The SLM Process: On the Need to Develop Machine Learning Models for Data Processing, In: Crystals, 2020.
- [20] Stutzman, C.; Przyjemski, A.; Nassar, A. R.: Effects of gas flow speed on bead geometry and optical emissions during laser powder bed fusion additive manufacturing, In: Rapid Prototyping Journal, 2023.
- [21] Felix, S.; Ray Majumder, S.; Mathews, H. K.; Lexa, M.; Lipsa, G.; Ping, X.; Roychowdhury, S.; Spears, T.: In situ process quality monitoring and defect detection for direct metal laser melting, In: Scientific reports, 2022.